Multijoint error compensation mediates unstable object control

Tyler Cluff,[1,2] **Aspasia Manos,**[2,3] **Timothy D. Lee,**[1,2] **and Ramesh Balasubramaniam**[1,2]
[1]*McMaster Integrative Neuroscience Discovery and Study (MiNDS), McMaster University, Hamilton, Ontario, Canada;*
[2]*Sensorimotor Neuroscience Laboratory, Department of Kinesiology, McMaster University, Hamilton, Ontario, Canada;*
and [3]*Department of Psychology, Neuroscience, and Behavior, McMaster University, Hamilton, Ontario, Canada*

Cluff T, Manos A, Lee TD, Balasubramaniam R. Multijoint error compensation mediates unstable object control. *J Neurophysiol* 108: 1167–1175, 2012. First published May 23, 2012; doi:10.1152/jn.00691.2011.—A key feature of skilled object control is the ability to correct performance errors. This process is not straightforward for unstable objects (e.g., inverted pendulum or "stick" balancing) because the mechanics of the object are sensitive to small control errors, which can lead to rapid performance changes. In this study, we have characterized joint recruitment and coordination processes in an unstable object control task. Our objective was to determine whether skill acquisition involves changes in the recruitment of individual joints or distributed error compensation. To address this problem, we monitored stick-balancing performance across four experimental sessions. We confirmed that subjects learned the task by showing an increase in the stability and length of balancing trials across training sessions. We demonstrated that motor learning led to the development of a multijoint error compensation strategy such that after training, subjects preferentially constrained joint angle variance that jeopardized task performance. The selective constraint of destabilizing joint angle variance was an important metric of motor learning. Finally, we performed a combined uncontrolled manifold-permutation analysis to ensure the variance structure was not confounded by differences in the variance of individual joint angles. We showed that reliance on multijoint error compensation increased, whereas individual joint variation (primarily at the wrist joint) decreased systematically with training. We propose a learning mechanism that is based on the accurate estimation of sensory states.

inverted pendulum; motor learning; motor variability; object manipulation; unstable dynamics

OBJECT MANIPULATION IS CENTRAL to many of the activities that we perform in daily life, and often, the objects that we control are unstable. Common examples include the waitress that balances a tray of drinks while maneuvering through a crowded restaurant or cyclists who navigate rush-hour traffic, avoiding pedestrians and vehicles while staying upright on their bicycles. In each of these tasks, the object is balanced at an unstable equilibrium and controlled through the interaction between the intrinsic object dynamics and applied forces (i.e., motor commands).

A number of studies have investigated unstable object control using an inverted pendulum (stick) balancing task (Cabrera and Milton 2002; Cabrera et al. 2004; Cluff and Balasubramaniam 2009; Cluff et al. 2009; Foo et al. 2000; Loram et al. 2009, 2011; Treffner and Kelso 1999) and have shown that performance is dependent on the accurate estimation of sensory states (Mah and Mussa-Ivaldi 2003; Mehta and Schaal 2002) and intermittent,

Address for reprint requests and other correspondence: T. Cluff, Laboratory of Integrative Motor Behavior (LIMB), Centre for Neuroscience Studies, Queen's University, Kingston, ON, Canada K7L 3N6 (e-mail: tyler.cluff@ queensu.ca).

time-delayed feedback control (Milton et al. 2009). The focus, however, has been to characterize the control mechanism at the hand, and we know little about the importance of joint recruitment and coordination processes in redundant object control tasks. This experiment examines motor learning in the stick-balancing task. We focus on two important aspects of coordination and characterize their role in motor skill acquisition: individual joint recruitment (task sharing) and multijoint error compensation.

The task-sharing perspective was pioneered by Bernstein's treatise on the coordination and control of voluntary movement (Bernstein 1967). Bernstein proposed that skilled motor behavior is acquired in three incremental stages that progress from learning to control to incorporating joint-space degrees of freedom (DOF) into task performance. Joint angle variances and paired joint angle excursions have been used extensively to evaluate the skill-dependent recruitment of individual joints (cf. Temprado et al. 1997). The recruitment of individual joints and the emergence of paired joint angle correlations have been reported for the acquisition of various motor skills, including ball bouncing (Broderick and Newell 1999), dart throwing (McDonald et al. 1989), simulated skiing (Vereijken et al. 1992), and the racquetball forehand shot (Southard and Higgins 1987).

The relationship between joint angle variance and outcome performance is confounded, however, by the equivocal mapping between individual joint trajectories and motion at the end effector (Lacquaniti and Soechting 1982; Polit and Bizzi 1978). It is therefore plausible that skilled performers engage a flexible multijoint control strategy that stabilizes task performance (Latash 2000; Latash et al. 2002, 2007; Yang and Scholz 2005). A very useful technique to investigate multijoint error compensation is the uncontrolled manifold (UCM) method (Scholz and Schoner 1999), which decomposes motor variance into two distinct components: *1*) variance that stabilizes performance (V_{UCM}) and *2*) variance that destabilizes performance (V_{ORT}). In the context of our study, V_{UCM} refers to joint angle configurations that map equivalently onto the task goal and stabilize the time-varying fingertip position (task-irrelevant variance). Conversely, V_{ORT} is the orthogonal joint variance component that destabilizes outcome performance (task-relevant variance). If the fingertip position is controlled by distributed error compensation, we expect the neural controller to permit variance in the UCM subspace (V_{UCM}) while constraining joint angle trajectories that jeopardize task performance (V_{ORT}).

We examined the joint angle variance structure using a link-segment model that mapped six independent joint angles onto the time profile of the fingertip (i.e., the sagittal plane coordinates of the balancing pivot). We hypothesized that unstable object control would be mediated by multijoint error compensation and that the selective constraint of destabilizing

joint angle variance would emerge with training. Indeed, we show that motor learning caused the selective control of destabilizing joint angle variance (V_{ORT}) but did not affect the flexible corrections that stabilized task performance (V_{UCM}). Finally, we provide evidence for distinct but overlapping motor learning processes. In early learning, we show that subjects stabilized performance by emphasizing corrections at the wrist joint (individual joint variation strategy) but favored distributed error compensation between joint angle trajectories later in training (multijoint error compensation strategy).

METHODS

Subjects. Eight healthy subjects (5 males, 3 females; age = 24.5 ± 2.4 yr) participated in the study. The subjects were right-handed, had normal or corrected vision, and reported no musculoskeletal or neurological disorders. Before the experiment, each subject attended a recruitment session that outlined the purpose of our study and time commitment. The protocol was approved by the McMaster University Research Ethics Board, and participants provided written informed consent. The participants were compensated for their time and could withdraw from the study at any time without penalty (none did so).

Protocol. We asked that subjects perform 20 balancing trials (2 blocks × 10 trials) during the initial recruitment/briefing session to familiarize themselves with the task. During the familiarization trials, the subjects balanced a cylindrical wooden dowel (stick) with different physical properties (length = 100 cm; diameter = 1.71 cm; mass = 150 g) than the stick used for the experiment and practice sessions (length = 62 cm; diameter = 1 cm; mass = 50 g). By increasing the moment of inertia of the stick about the balancing pivot, we provided additional time for corrective limb displacements. We reasoned that familiarization trials would ensure that subjects understood the task but that this would transfer marginally to the experiment (cf. Braun et al. 2009). We recorded each subject's preferred foot placement to ensure the balancing posture was consistent between trials and learning sessions.

Each subject attended daily practice sessions conducted at the laboratory. Because the length of each trial (balance until failure) varied by participant and across practice sessions, there was not a fixed number of practice trials. Instead, the subjects practiced for 30 min per session. We maintained a log to ensure that each subject satisfied these practice requirements.

Motor learning was monitored in four experimental sessions (~90 min, including subject preparation time) that we conducted every fourth day during the 2-wk training period. The experimental sessions consisted of 20 trials (2 blocks × 10 trials) that ended when the subject dropped the stick. We instructed subjects to balance the stick for as long as possible (balance until failure) and maintained consistent postural alignment by ensuring that subjects aligned their feet with their preferred stance. If the preferred balancing stance was not maintained during trial performance, we repeated data collection for that trial. Individual trials were separated by a minimum of 30 s, and blocks of trials were separated by a 5-min rest period. We supplemented the allotted rest breaks at the subjects' request to alleviate discomfort due to visual strain and physical or attentional fatigue.

Equipment and apparatus. We recorded body segment kinematics using 14-mm spherical reflective markers positioned over surface anatomical landmarks that provide an approximation to the joint centers of rotation (ankle joint: lateral malleolus; knee joint: lateral femoral condyle; hip joint: greater trochanter; shoulder joint: inferior to the lateral aspect of the acromion process; elbow joint: lateral humeral condyle; wrist joint: styloid process of the radius). We also attached 14-mm reflective markers to the top and bottom of the stick. The marker coordinates were recorded at a sampling rate of 750 Hz using a 10-camera VICON T-40 motion capture system (Lake Forest, CA).

Data reduction. The three-dimensional data were reconstructed and autolabeled off-line by using link-segment models constructed for each

subject with the VICON Nexus software. We low-pass filtered the data (10-Hz effective cutoff, 2nd-order, dual-pass Butterworth) in Matlab (R2009a; The MathWorks, Natick, MA). A bidirectional digital filter was used to minimize artificial phase shifts induced by the filtering algorithm.

Angle calculations. We restricted the analysis to the right-side (i.e., balancing side) sagittal plane joint kinematics and calculated the ankle, knee, hip, shoulder, elbow, and wrist joint angles at each data sample using the filtered marker coordinates. The link-segment model and marker placements are outlined in Fig. 1. We calculated sagittal plane joint angles using the formula
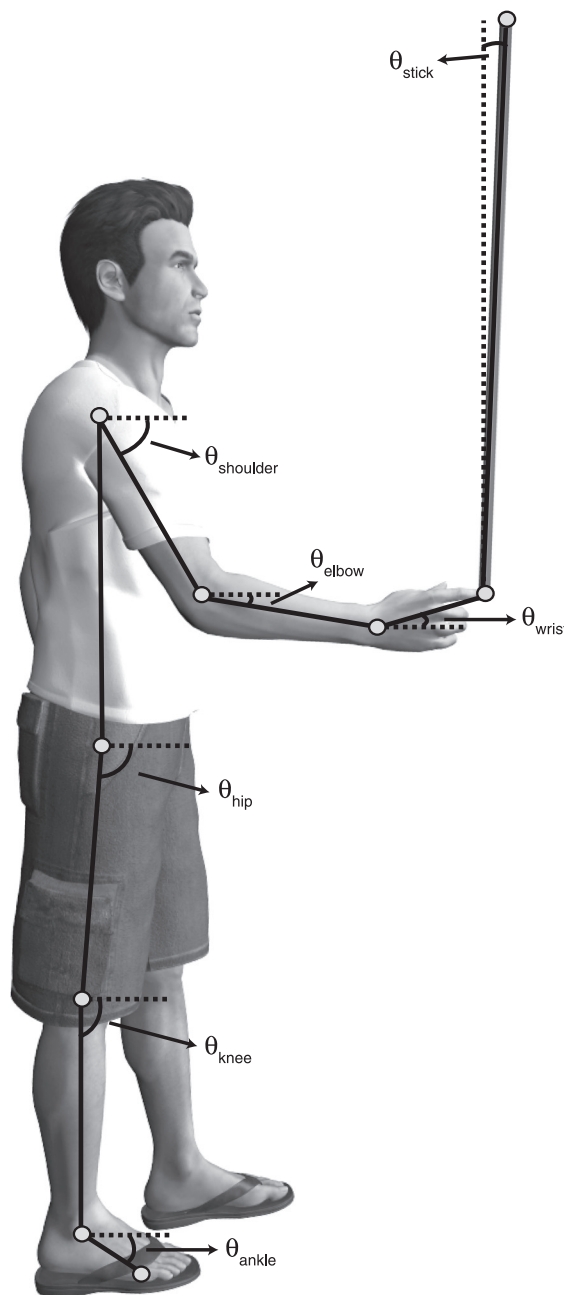
Fig. 1. Schematic of the experimental setup showing the reflective markers (circles) used to construct the link-segment model (solid line). Sagittal plane joint angles (θ) were calculated for the ankle, knee, hip, shoulder, elbow, and wrist joints. Joint angles were defined relative to the right horizontal (dashed horizontal lines), and the angle of the stick was defined relative to the vertical (dashed vertical line).

$$\theta_i = \arctan2\left(\frac{\vec{u} \times \vec{v}_i}{\vec{u} \cdot \vec{v}_i}\right),$$

where θ_i corresponds to the joint angle about the ith joint, $\vec{u}$ corresponds to the unit vector directed along the right horizontal, and $\vec{v}$ is the unit vector corresponding to the limb segment proximal to the ith joint of the link-segment model. The joint angles were defined relative to the right horizontal with positive angles in the counterclockwise direction. We used the same formula to calculate the stick angle with respect to vertical; however, for stick angle calculations, $\vec{u}$ is the unit vector directed along the upward vertical and $\vec{v}$ is the unit vector of the sagittal plane stick coordinates. Positive stick angles were defined in the counterclockwise direction. We removed the first and last 3 s of trial data to confine the analysis to steady-state balancing processes and avoid transient adjustments at the onset and just before the end of each trial.

Mean balancing time and root-mean-square vertical stick angle. We computed the mean balancing time as the arithmetic mean trial length performed by subjects in each experimental session. In addition to the mean balancing time measure, we computed subject-specific root-mean-square (RMS) stick angles for each experimental session. We used these dependent measures to examine changes in stick-balancing performance.

Variance of individual joint angle excursions. We calculated the variance of angular joint excursions to examine changes in the recruitment of individual joints during motor learning. We first deter-

mined the occurrence of successive corrections based on local maxima in the angular stick profile. For each trial, we partitioned the joint angle kinematics into time profiles with beginning and end points defined by these local maxima. Each corrective displacement was normalized to 101 points (%correction) by linear interpolation. For every subject, we calculated the variance of individual joint angles for corrective movements performed within each trial and averaged this measure across trials within each session.

Correlations between individual joint excursions. To investigate change in the coupling of individual joints, we calculated the zero-lag cross-correlation coefficient between all combinations of paired joint angle time series. The cross-correlation coefficients were calculated for each individual trial and then averaged across trials in each session. The sign of the cross-correlation specifies the direction of coupling, whereas the magnitude indicates the degree of coupling between body segments; the more independent the joint motions, the closer the coefficient would be to zero. Negative correlations reflect error compensation between paired joint angle trajectories.

Joint variance and its relationship to performance stability. The mathematical methods for the UCM analysis have been described elsewhere in detail (Scholz and Schoner 1999). Our initial step was to specify a link-segment model that related individual sagittal plane joint angles to the hypothesized finger coordinate control variables (Milton et al. 2009). We constructed a link-segment model that consisted of six sagittal plane joint angles. The link-segment model relating the joint configuration to the sagittal plane finger coordinates at each sample was

$$\begin{bmatrix} x_{\text{finger}} \\ y_{\text{finger}} \end{bmatrix} = \begin{bmatrix} l_{\text{shank}}\cos\theta_{\text{ankle}} + l_{\text{thigh}}\cos\theta_{\text{knee}} + l_{\text{trunk}}\cos\theta_{\text{hip}} + l_{\text{upper arm}}\cos\theta_{\text{shoulder}} + l_{\text{forearm}}\cos\theta_{\text{elbow}} + l_{\text{hand}}\cos\theta_{\text{wrist}} \\ l_{\text{shank}}\sin\theta_{\text{ankle}} + l_{\text{thigh}}\sin\theta_{\text{knee}} + l_{\text{trunk}}\sin\theta_{\text{hip}} + l_{\text{upper arm}}\sin\theta_{\text{shoulder}} + l_{\text{forearm}}\sin\theta_{\text{elbow}} + l_{\text{hand}}\sin\theta_{\text{wrist}} \end{bmatrix},$$

where θ_{ankle}, θ_{knee}, . . . , θ_{wrist} are the sagittal plane joint angles, and l_{shank}, l_{thigh}, . . . , l_{hand} are the segment lengths that we calculated from marker coordinate data averaged over the first 3 s

of each trial. The individual joint angles were mapped onto the time-varying finger coordinates using the Jacobian matrix $J(\theta) = \partial F/\partial\theta_i$:

$$J(\theta) = \begin{bmatrix} -l_{\text{shank}}\sin\theta_{\text{ankle}} & -l_{\text{thigh}}\sin\theta_{\text{knee}} & -l_{\text{trunk}}\sin\theta_{\text{hip}} & -l_{\text{upper arm}}\sin\theta_{\text{shoulder}} & -l_{\text{forearm}}\sin\theta_{\text{elbow}} & -l_{\text{hand}}\sin\theta_{\text{wrist}} \\ l_{\text{shank}}\cos\theta_{\text{ankle}} & l_{\text{thigh}}\cos\theta_{\text{knee}} & l_{\text{trunk}}\cos\theta_{\text{hip}} & l_{\text{upper arm}}\cos\theta_{\text{shoulder}} & l_{\text{forearm}}\cos\theta_{\text{elbow}} & l_{\text{hand}}\cos\theta_{\text{wrist}} \end{bmatrix}.$$

Our second step was to compute the linear approximation of individual joint angles onto the invariant joint configuration subspace (UCM). This step required specification of the referent joint configuration at each normalized time sample. For each trial, the local angular stick maxima were used to partition joint motion profiles into successive corrections (see *Variance of individual joint angle excursions*). The joint angle time series were ensemble-averaged at each normalized sample to determine the time-varying referent joint configurations. Our method is a within-trials UCM analysis that examines distributed, online error compensation between joint angles (Ranganathan and Newell 2008; Scholz et al. 2003).

We used the referent joint configuration to compute the UCM at each normalized time sample. The linear approximation to the UCM was calculated by determining the null-space of the Jacobian matrix with respect to the referent joint configuration. The null-space of the Jacobian matrix was calculated by singular value decomposition in Matlab. We then calculated the angular deviation matrix by subtracting each joint angle from its respective referent angle, projected it onto the null-space of the Jacobian, and computed the square-norm. We used this projection to provide a scalar estimate of how consistent the joint-space configuration was with the referent finger coordinate at that time sample; we used the complement to estimate the extent to which the joint configuration destabilized the instantaneous finger coordinates. The variances within the UCM (V_{UCM}) and orthogonal

subspace (V_{ORT}) were normalized to the dimension of the subspace ($\text{DOF}_{\text{UCM}} = 4$, $\text{DOF}_{\text{ORT}} = 1$), the number of samples ($n = 101$ samples), and the number of corrections, which varied from trial to trial. We used the UCM ratio, defined as variability within the UCM relative to the orthogonal joint configuration subspace ($\text{UCM}_{\text{ratio}} = V_{\text{UCM}}/V_{\text{ORT}}$), to determine whether learning evoked multijoint error compensation. A $\text{UCM}_{\text{ratio}}$ value >1 would demonstrate that selective error compensation is used to stabilize the time-varying finger coordinate profile.

Decomposition of multijoint covariation and individual joint variation strategies. A potential caveat of the UCM analysis is that the joint angle variance structure may arise from the inequality of variances between measured joint angles (individual joint variation) and not from joint angle deviations that compensate for one another (multijoint error compensation) (cf. the proof in Appendix B, Yen and Chang 2010). To determine the effect of individual joint angle variances, we computed the UCM ratio of a surrogate data set formed by joint angle permutation among all corrections performed by subjects in each experimental session. The joint angle permutation was performed at each normalized time sample by combining the wrist joint angle with every measured ankle, knee, hip, shoulder, and elbow joint angle in all possible combinations. The surrogate data set removed covariation between joint angles, but left the individual joint angle variances the same as in the original data set. If the UCM

analysis on this surrogate data set revealed selective stabilization of the fingertip position (InV = UCM_{ratio} of the surrogate data set), this result would show that the calculated joint variance structure was confounded by the inequality of individual joint angle variances. To determine the amount of fingertip stabilization that arose from multijoint error compensation (CoV), we took the difference between the UCM_{ratio} of the original and surrogate data sets (CoV = UCM_{ratio} − InV). The CoV measure specifies the amount of covariation used to stabilize the time-varying fingertip position. A CoV value of 0 would show the joint angle variance structure in the UCM analysis arose from the inequality of individual joint angle variances. Conversely, a CoV value equal to the UCM_{ratio} from the original data set would show that subjects use selective multijoint compensation to stabilize the fingertip position.

To further characterize the contribution of the individual joint variation and multijoint covariation strategies, we computed the relative stabilization index (RSI = CoV/UCM_{ratio}). An RSI value of 1 would demonstrate that subjects use multijoint covariation to stabilize the time-varying fingertip position, whereas an RSI value of 0 would show that subjects stabilize the stick using individual joint recruitment. An RSI value of 0.5 would show that subjects stabilize the stick using equal contributions from the individual joint and multijoint covariation strategies.

Relationship between the variability ratio and performance. We performed linear regression analysis in each experimental session and calculated Pearson's product-moment correlation coefficients to examine the relationship between balancing time and the UCM_{ratio}. Positive correlation between the UCM_{ratio} and mean balancing time would demonstrate that performance is dependent on the degree of error compensation between joints. We were interested in the relationship between coordinated feedback control and stick-balancing performance.

Statistical analysis. For every dependent measure, we averaged individual subject data across trials performed in each session. We used separate one-way repeated-measures analysis of variance (ANOVA) to quantify changes in balancing time and the RMS vertical stick angle across experimental sessions (4 levels: *sessions 1–4*). Similarly, we performed separate one-way repeated-measures ANOVA for each individual joint angle (ankle, knee, hip, shoulder, elbow, and wrist joint) to determine whether the variances of joint excursions were affected by motor learning. In addition, we performed two-way repeated-measures ANOVA to determine if the organization of angular joint variance (2 levels: V_{UCM} and V_{ORT}) differed between experimental sessions (4 levels: *sessions 1–4*). Finally, we log-transformed the UCM_{ratio} [UCM_{ratio} = $\ln(UCM_{ratio})$] to correct for deviations from normality (Kolmogorov-Smirnov test, $P < 0.05$) and contrasted it across sessions using a one-way repeated-measures ANOVA. For the UCM-joint angle permutation analysis, we performed separate repeated-measures ANOVA for the CoV and RSI variables. All post hoc mean comparisons were performed using paired *t*-tests with Holm-Bonferroni corrections (Holm 1979). We performed the statistical analyses in PASW (version 18.0; SPSS,

Chicago, IL) with the significance level set to $\alpha = 0.05$. Pairwise mean differences and corrected *P* values are reported in the text and Figs. 2–6.

RESULTS

Mean balancing time and RMS stick angle. Mean balancing time showed a marked learning effect [$F_{(3, 21)} = 22.86$, $P < 0.001$, Fig. 2*A*], and post hoc comparisons confirmed that balancing time increased across training sessions (*session 4* > *sessions 1* and *2*, *session 3* > *session 1*; all $P < 0.05$). Similarly, we found the vertical stick angle was more stable late in the learning paradigm relative to the onset of training [$F_{(1.38, 9.62)} = 5.44$, $P < 0.05$, Fig. 2*B*]. The effect was confirmed by post hoc analysis, which demonstrated that the RMS stick angle decreased across experimental sessions (*session 4* > *sessions 1* and *2*; all $P < 0.05$). In the following sections, we interpret individual joint recruitment and multijoint error compensation mechanisms in relation to the performance changes that accompanied motor learning.

Individual joint angle variances and the relationship between joint excursions. The *top* panels of Fig. 3 show the variability of the ankle (*A*), knee (*B*), and hip joints (*C*) ensemble-averaged across subjects. In contrast to the variance of lower limb joints, the *bottom* panels of Fig. 3 show that shoulder (*D*), elbow (*E*), and wrist excursions (*F*) were substantially more variable. The statistical analysis demonstrated that whereas the variance of ankle [$F_{(2.09, 14.65)} = 3.39$, $P > 0.05$], knee [$F_{(1.16, 8.82)} = 1.16$, $P > 0.05$, Huynh-Feldt correction], hip [$F_{(3, 21)} = 2.26$, $P > 0.05$], shoulder [$F_{(3, 21)} = 2.47$, $P > 0.05$], and elbow excursions [$F_{(3, 21)} = 1.69$, $P > 0.05$] were approximately constant, learning caused a reduction in wrist joint variance [$F_{(3, 21)} = 5.58$, $P < 0.001$]. Post hoc comparisons confirmed that the variability of wrist joint excursions decreased across training sessions (*session 4* < *session 1*; $P < 0.05$). To verify that each joint was engaged in task performance, we used directional *t*-tests that compared the individual joint angle variances in each session with a test value of 0 rad. In every experimental session, we found that each individual joint was recruited for task performance (single-sided *t*-tests, all $P < 0.05$).

We subsequently performed cross-correlation analyses to determine whether changes in performance were related to straightforward covariation between paired joint angle trajectories. Before statistical analysis was performed, the zero-lag cross-correlation coefficients were log-transformed [$r = \ln(r)$] to correct for deviations from normality (Kolmogorov-Smirnov test, $P < 0.05$). We found that performance was subserved

Fig. 2. Comparison of performance by experimental session. *A*: mean balancing time. *B*: root-mean-square (RMS) stick angle. RMS stick angle decreased as a function of practice, demonstrating that subjects more effectively stabilized the stick. Data are plotted as grand-ensemble means across subjects. Error bars represent the within-subjects SE. *$P < 0.05$; **$P < 0.01$; ***$P < 0.001$.
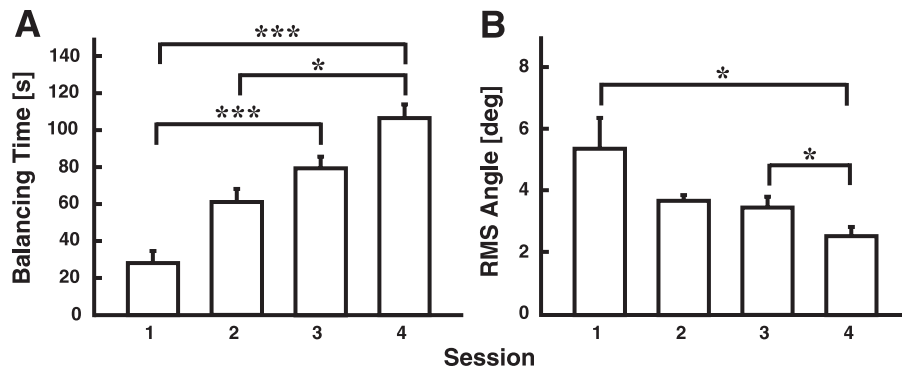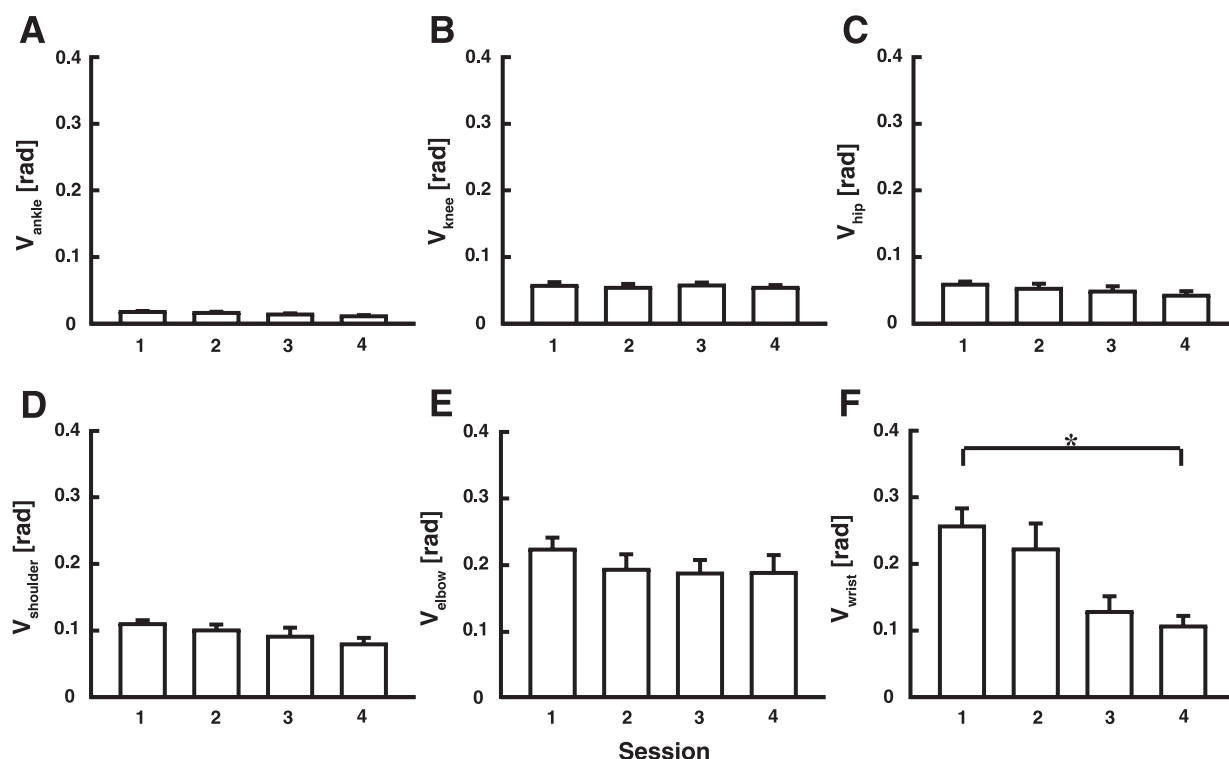
Fig. 3. Variance (V) of joint angle excursions at the ankle (*A*), knee (*B*), hip (*C*), shoulder (*D*), elbow (*E*), and wrist joints (*F*) by experimental session. Joint angle variance was small in the lower relative to the upper extremity joints. Each bar denotes the between-subjects standard deviation across trials performed in that session. Error bars represent the within-subjects SE. *$P < 0.05$.

by a complex set of correlated joint angle excursions. Table 1 shows the correlation between individual joint excursions was at best moderate (in most cases $r \ll 0.70$) and unaffected by training (all $P > 0.05$). To further understand the interdependence of the individual joint kinematics, we performed a within-trials UCM analysis, which allowed us to interpret differences in the joint angle variance structure evoked by motor learning.

Ratio of variability: structure of joint configuration variability related to the stability of the finger coordinate control variable. Figure 4 plots V_{UCM} (*A*) and V_{ORT} (*B*) derived from the link-segment model (Fig. 1) that related the independent

Table 1. *Average zero-lag cross-correlation between paired joint angle trajectories*

Joint Pair	Session 1	Session 2	Session 3	Session 4
Ankle-knee	0.41 ± 0.20	0.29 ± 0.12	0.50 ± 0.22	0.44 ± 0.22
Ankle-hip	0.16 ± 0.14	0.20 ± 0.12	0.20 ± 0.20	0.19 ± 0.18
Ankle-shoulder	0.20 ± 0.20	0.29 ± 0.10	0.33 ± 0.08	0.20 ± 0.18
Ankle-elbow	0.15 ± 0.14	0.19 ± 0.12	0.27 ± 0.10	0.19 ± 0.12
Ankle-wrist	0.22 ± 0.12	0.16 ± 0.16	0.16 ± 0.14	0.16 ± 0.10
Knee-hip	0.27 ± 0.36	0.26 ± 0.28	0.28 ± 0.36	0.28 ± 0.14
Knee-shoulder	0.38 ± 0.20	0.43 ± 0.18	0.46 ± 0.20	0.41 ± 0.14
Knee-elbow	0.50 ± 0.18	0.53 ± 0.22	0.52 ± 0.22	0.51 ± 0.14
Knee-wrist	0.16 ± 0.28	0.16 ± 0.24	0.18 ± 0.20	0.17 ± 0.08
Hip-shoulder	0.19 ± 0.20	0.20 ± 0.16	0.15 ± 0.18	0.24 ± 0.14
Hip-elbow	0.40 ± 0.16	0.30 ± 0.18	0.29 ± 0.18	0.45 ± 0.10
Hip-wrist	0.24 ± 0.18	0.21 ± 0.10	0.24 ± 0.14	0.28 ± 0.10
Shoulder-elbow	0.52 ± 0.12	0.62 ± 0.14	0.67 ± 0.04	0.62 ± 0.10
Shoulder-wrist	0.11 ± 0.12	0.15 ± 0.18	0.09 ± 0.22	0.14 ± 0.16
Elbow-wrist	0.46 ± 0.14	0.44 ± 0.18	0.26 ± 0.24	0.46 ± 0.10

Results are between-subjects averages ± 95th-centile confidence interval of the mean (all $P > 0.05$).

joint angles to the finger coordinate control variable. Two-way ANOVA revealed that the variance distributed along the UCM subspace (V_{UCM}, Fig. 4*A*) was significantly larger [$F(1, 7) = 7.42$, $P < 0.03$] than the variance in the orthogonal direction (V_{ORT}, Fig. 4*B*). In addition, there was a significant session-by-variance component interaction [$F(3, 21) = 8.46$, $P = 0.001$] that we decomposed by planned univariate comparisons (simple main effects). The planned comparisons demonstrated that although there was no change in V_{UCM} [$F(3, 21) = 0.64$, $P > 0.05$, Fig. 4*A*], training caused a substantial reduction of V_{ORT} [$F(3, 21) = 8.00$, $P < 0.001$, Fig. 4*B*].·· V_{ORT} was greatest at the outset of training but decreased monotonically (all $P < 0.05$) to demonstrate that multijoint error compensation minimized the deleterious effects of joint angle variance. The effect is further summarized by the covariance ellipses in Fig. 5, which show the systematic reduction of V_{ORT} across experimental sessions. We confirmed this effect using the UCM_{ratio}, which was defined as the relative variance per DOF in each joint variance subspace. The UCM_{ratio} increased with training to show that subjects constrained joint configurations that jeopardized task performance [$F(3, 21) = 12.68$, $P < 0.001$, Fig. 4*C*]. The results confirmed our experimental hypothesis and demonstrated that learning led to flexible multijoint corrections that selectively minimized destabilizing joint angle variance.

To ensure the joint variance structure calculated by the UCM analysis arose from multijoint compensation and not individual joint variation, we performed a combined UCM-permutation analysis using the surrogate data set that consisted of the wrist joint angle paired with every combination of ankle, knee, hip, shoulder, and elbow joint angle at each normalized time sample. We calculated the UCM_{ratio} of the permuted data set
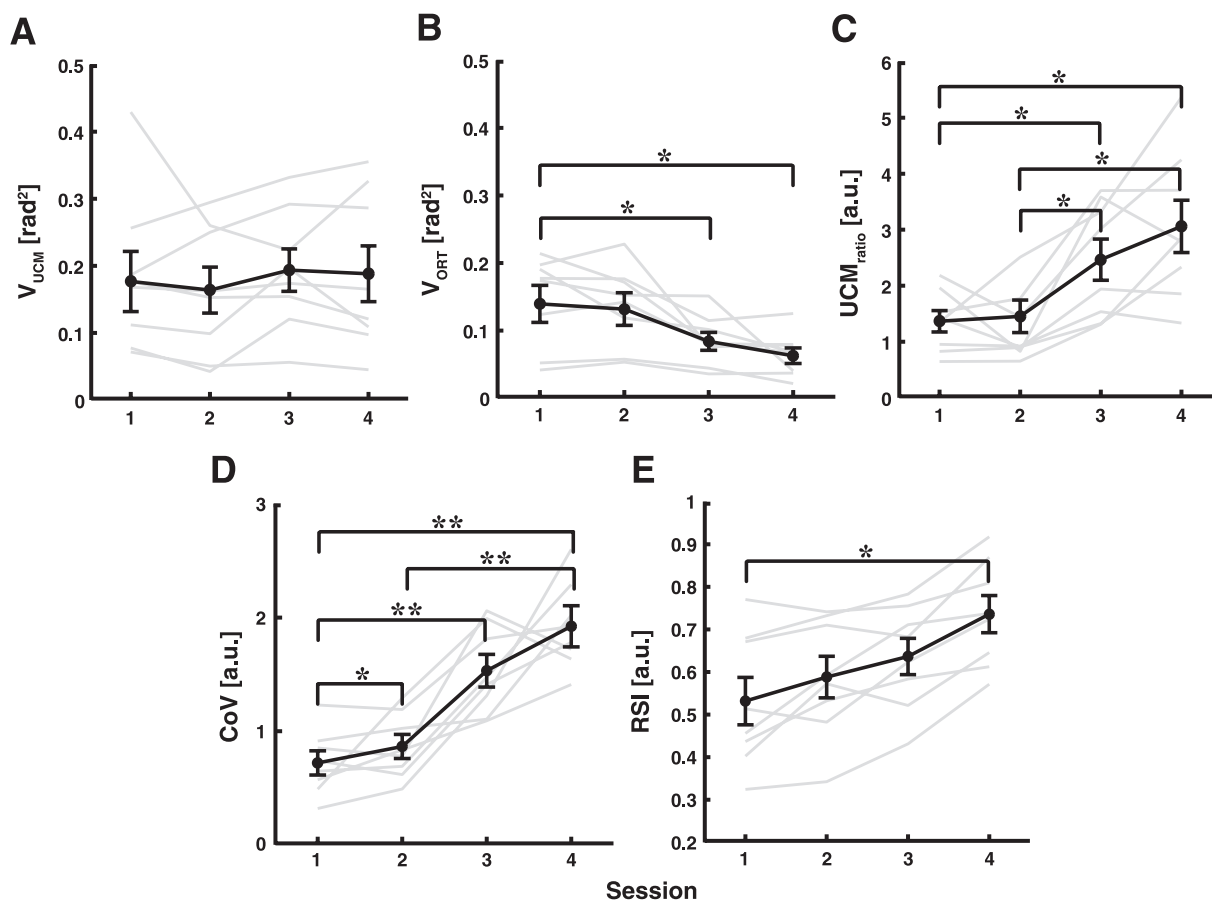
Fig. 4. Mean joint configuration variability per degree of freedom aligned on the uncontrolled manifold (V_{UCM}; *A*) and the orthogonal subspace (V_{ORT}; *B*), and the ratio of variance aligned on the UCM relative to the orthogonal joint configuration subspace (UCM_{ratio}; *C*). In *D* and *E*, the results of the surrogate UCM analysis are contrasted with the original UCM analysis. Multijoint error compensation (CoV) increased across training sessions (*D*), which demonstrates that motor learning decreased emphasis on the individual joint recruitment strategy, since CoV accounted for a greater proportion of the joint angle variance structure across training sessions (relative stabilization index, RSI; *E*). Gray lines correspond to individual subject data; black lines plot the average across subjects. Error bars represent the within-subjects SE. *$P < 0.05$; **$P < 0.01$.

(InV) and found the amount of multijoint CoV by subtracting InV from the UCM_{ratio} of the original data set. One-way ANOVA showed that training caused a systematic increase in multijoint covariance [$F(1.45, 10.17) = 53.32$, $P < 0.001$, Huynh-Feldt correction]. We confirmed this result using post hoc comparisons and found that multijoint error compensation was smallest at the start of training but increased across experimental sessions (all $P < 0.05$, Fig. 4*D*). Thus, with training, the subjects used flexible multijoint corrections that stabilized the time-varying fingertip position. We further analyzed the contribution from individual joint and multijoint compensation strategies by computing the RSI, which we defined as the ratio between multijoint CoV and the UCM_{ratio} of the original data set. We found that motor learning influenced the RSI [$F(3, 21) = 5.86$, $P < 0.01$], and post hoc comparisons showed that the RSI was greater in the last relative to the first experimental session (*session 4* > *session 1*, $P < 0.05$). In summary, we found that subjects relied increasingly on the multijoint covariation strategy (CoV) and less on the individual joint variation strategy (InV) across training sessions (Fig. 4, *D* and *E*).

Relationship between error compensation mechanisms and performance. We performed a linear regression analysis and found a significant linear relationship between the UCM_{ratio} and stick-balancing performance (Fig. 6). In each experimental session, the subjects who controlled multijoint kinematic error performed best at the stick-balancing task [*session 1*: $F(1, 6) = 8.07$, $P < 0.05$, $R^2 = 0.573$; *session 2*: $F(1, 6) = 15.31$, $P < 0.01$, $R^2 = 0.718$; *session 3*: $F(1, 6) = 8.33$, $P < 0.05$, $R^2 = 0.580$; *session 4*: $F(1, 6) = 26.63$, $P < 0.01$, $R^2 = 0.804$].

DISCUSSION

We undertook this experiment to examine changes in the coordination and control of individual joints during the acquisition of an unstable object control task. We examined individual joint recruitment patterns and performed a within-trials UCM analysis that examined changes in the structure of joint angle variance. We focused on the differential management of multijoint variance that stabilized (V_{UCM}) and destabilized (V_{ORT}) the time-varying fingertip position with the objective to characterize the coordination mechanisms underlying redundant unstable object control tasks. This study is the first to differentiate skill-related differences in multijoint covariation and individual joint recruitment strategies in an unstable object control task.

A key finding in this experiment was that the variance of individual joint angle excursions did not increase with learning, and in contrast, we found a systematic reduction in wrist joint variance across training sessions. This result was con-
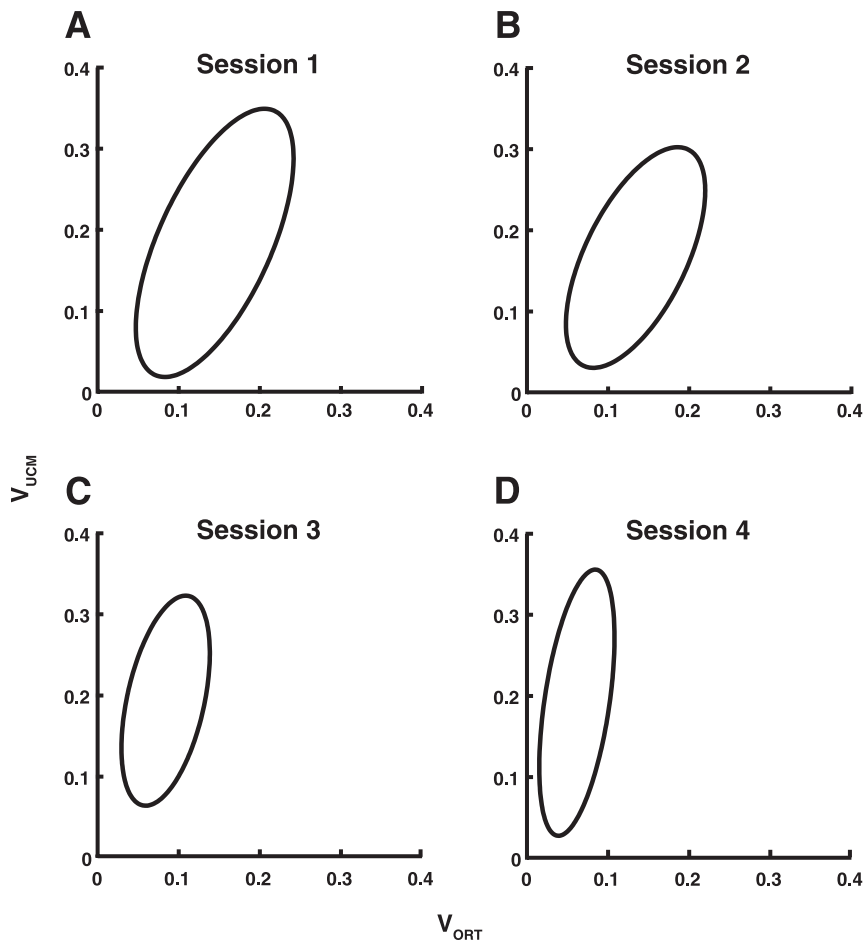
Fig. 5. Motor learning caused the selective reduction of joint configurations that destabilized task performance. The covariance ellipses show the between-subjects distribution of joint configuration variance for each session. The data are presented as the ensemble-average across subjects for repeated corrections performed in individual trials. The covariance ellipses in *A* and *B* show covariation between individual joint configurations in *sessions 1* and *2*, whereas *C* and *D* show progressive strengthening of error compensation between joints (V_{UCM}) with reduction of the orthogonal variance component (V_{ORT}) in *sessions 3* and *4*.

firmed by the combined UCM-joint angle permutation analysis, which showed that stabilization arising from the individual joint variation strategy decreased systematically across experimental sessions. Another important result was that the zero-lag cross-correlation coefficient between paired joint angle
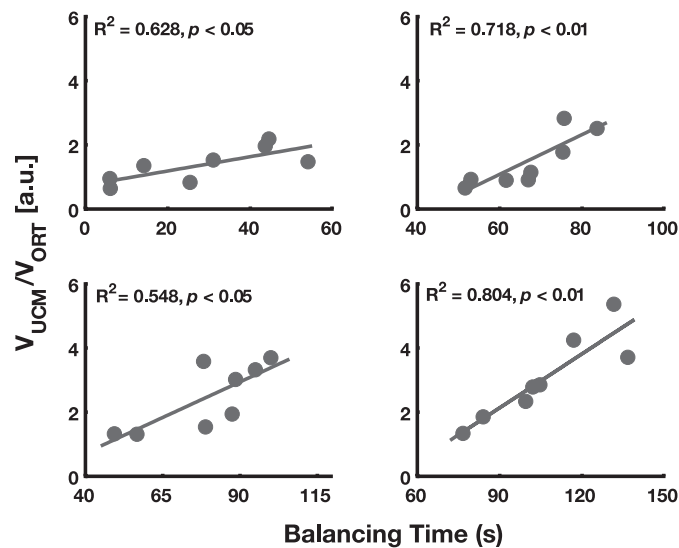
Fig. 6. Relationship between mean balancing time and the variability ratio (V_{UCM}/V_{ORT}). V_{UCM}/V_{ORT} was correlated with the mean balancing time such that subjects who selectively minimized V_{ORT} performed better at the stick balancing task. Circles represent individual subject data ensemble-averaged across corrections performed in each experimental session.

trajectories was of moderate strength, at best, but was in general well below 0.5, which demonstrates that correlated joint recruitments were too weak for any one pair of joints to have underscored the incremental changes in task performance. In summary, our results do not directly support the argument that motor learning consists of three incremental stages differentiated by the initial freezing (or equivalently, rigid control) and progressive recruitment (or flexible control) of individual joints (Bernstein 1967), but corroborate growing evidence which shows that skill acquisition in multijoint motor tasks involves flexible, task-dependent joint recruitment strategies (Buchanan and Horak 1999; Konczak et al. 2009).

There are two mechanisms that may account for the decrease in wrist joint variance reported in this study. The first mechanism is that destabilizing wrist displacements may have arisen due to the inappropriate control of interaction torques generated during the upper limb corrections (Atkeson 1989); however, the mass of the stick (50 g) would have had negligible effect on the upper limb and would likely have been offset by neural mechanisms that compensate for the complexity of upper limb joint motion (Gribble and Scott 2002; Kurtzer et al. 2008). The second mechanism is that the wrist joint may have compensated for balancing errors in early learning and was recruited progressively less as participants learned the stick-balancing task. A similar compensatory mechanism has been proposed for the reduction of lower limb joint variance when participants learn to control posture in the presence of sinusoidal platform oscillations (Ko et al. 2001).

The reduction of wrist joint variance in this study is consistent with motor learning experiments that examined joint angle variance (Anderson and Sidaway 1994; Young and Marteniuk 1998) in both single-joint (Gabriel 2002) and multijoint tasks (Timmann et al. 2001) but is difficult to interpret because the redundancy of multijoint motion does not provide any straightforward mapping between joint angle trajectories and the kinematics of the end-effector (Latash 2000). In view of this limitation, we performed a UCM analysis that probed the complex structure of the multijoint kinematics.

A noteworthy finding was the differential management of joint angle variance that developed across experimental sessions. We reported a progressive decrease in overall joint angle variance and demonstrated that this effect was caused by the selective reduction of variance in the subspace of destabilizing joint angle configurations (V_{ORT}). Learning caused a systematic increase in the UCM_{ratio}, which reflects error compensation between joints so that if the contribution of one joint perturbed the instantaneous finger position, the configuration of other joints was modified to stabilize it. We also performed a correlation analysis and found that the magnitude of the UCM_{ratio} was an important determinant of stick-balancing performance, which demonstrates that the selective and progressive constraint of V_{ORT} was associated with better task performance.

A number of studies have shown that skill acquisition changes the partitioning of motor variance between task-relevant (V_{ORT}) and task-irrelevant (V_{UCM}) dimensions, but there has been a lack of consensus as to how motor learning affects the structural distribution of variance in redundant motor tasks (Latash et al. 2007). For example, studies have reported larger (Domkin et al. 2002), equal (Domkin et al. 2005), and smaller decreases (Yang and Scholz 2005) in V_{UCM} relative to simultaneous decreases in V_{ORT}. These considerations have prompted a number of explanations, including optimization criteria imposed to constrain motor responses (Domkin et al. 2002, 2005) and a lack of novelty or insufficient training (Domkin et al. 2002).

In contrast, we demonstrated that motor learning evoked the selective reduction in V_{ORT}, and our results are consistent with the Frisbee task investigated by Yang and Scholz (2005), where subjects exhibited less motor variance on average, and this reduction was largely confined to solutions that jeopardized the outcome of the toss. In the present study, we reported a similar reduction in joint angle variance, but our effect arose from the constraint of destabilizing joint configurations combined with the simultaneous reduction of variance at the wrist joint. In consideration of these findings, two important questions are, what is the significance of V_{ORT}, and why did it decrease by more than 50% across training sessions?

The goal-specific processing of sensory feedback is a key attribute of skilled motor behavior (Scott 2004). The confluence between sensory feedback and voluntary control processes has been formalized by the optimal feedback control framework (OFC) (Todorov and Jordan 2002), which suggests that the central nervous system constructs modifiable, task-dependent feedback control policies that transform sensory feedback into optimal motor responses (Diedrichsen et al. 2010). According to OFC, successful behavior is dependent on two interrelated neural processes: state estimation and feedback control. It has been demonstrated that state estimation processes rely on neural representations that encode the physical properties of our limbs (Flanagan

and Lolley 2001), environment (Gribble and Scott 2002), and manipulated objects (Mah and Mussa-Ivaldi 2003), and a common argument is that these force-motion models are acquired before the development of task-specific feedback control policies (Flanagan et al. 2003).

In our study, it is possible that the progressive reduction in V_{ORT} reflects the acquisition of accurate state estimation processes. This would situate our data in the context of work by Mehta and Schaal (2002), who used visual feedback occlusion (600 ms) and perturbing force pulses to show that state estimation processes are intimately linked to human balance control. We argue that the systematic reduction in wrist joint variance is well explained by Mehta and Schaal's (2009) stick-balancing experiment: because the hand is the terminal segment of the upper limb and possesses the least segmental inertia, a high-gain feedback-corrective mechanism could enable rapid, independent corrections to be performed at the wrist joint. As subjects learned the transformation between applied upper limb forces and the motion of the stick, the corresponding motor commands would reflect the state of the stick, reduce error, and thereby decrease emphasis on these compensatory wrist displacements. This learning mechanism was supported by the outcome of the UCM-joint angle permutation analysis, which demonstrated that the reduction in individual joint variation was accompanied by a concomitant increase in multijoint covariation: as subjects learned the task, they relied less on the control of individual joints and more on distributed error compensation, and this transition was accompanied by improved performance. Similar control mechanisms have been proposed when participants learn to control posture in the presence of sinusoidal platform oscillations (Ko et al. 2001) and during the stabilization of the vertical ground reaction force in externally paced human hopping tasks (Yen and Chang 2010). For example, Yen and Chang (2010) performed the same permutation analysis and found that vertical force stabilization relied less on interjoint coordination at high hopping frequencies and more on the selection of appropriate ankle joint torques. Collectively, these studies suggest individual joint variation may be more important for difficult task conditions (Yen and Chang 2010) or during the acquisition of novel motor skills (Ko et al. 2001).

In conclusion, we have shown that multijoint error compensation is a key factor in unstable object control tasks and that the preferential control of destabilizing joint angle variance engenders incremental changes in performance. Our data have implications in understanding the coordination processes underlying multijoint object control tasks, and we expect this approach will be a fundamental step in linking the higher order structural properties of motor variance to the estimation and control processes acquired during motor learning.

AUTHOR CONTRIBUTIONS

Author contributions: T.C. and R.B. conception and design of research; T.C. performed experiments; T.C. and A.M. analyzed data; T.C., A.M., T.D.L., and R.B. interpreted results of experiments; T.C. prepared figures; T.C., A.M., T.D.L., and R.B. drafted manuscript; T.C., A.M., T.D.L., and R.B. edited and revised manuscript; T.C., A.M., T.D.L., and R.B. approved final version of manuscript.

REFERENCES

Anderson D, Sidaway B. Coordination changes associated with practice of a soccer kick. *Res Q Exerc Sport* 65: 93–99, 1994.

Atkeson CG. Learning arm kinematics and dynamics. *Annu Rev Neurosci* 12: 157–183, 1989.

Bernstein NA. The coordination and regulation of movements. Oxford: Pergamon, 1967.

Braun DA, Aersten A, Wolpert DM, Mehring C. Motor task variation induces structural learning. *Curr Biol* 19: 352–357, 2009.

Broderick MP, Newell KM. Coordination patterns in ball bouncing as a function of skill. *J Mot Behav* 31: 165–188, 1999.

Buchanan JJ, Horak FB. Emergence of postural patterns as a function of vision and translation frequency. *J Neurophysiol* 81: 2325–2339, 1999.

Cabrera JL, Milton JG. On-off intermittency in a human balancing task. *Phys Rev Lett* 89: 158702, 2002.

Cabrera JL, Milton JG. Human stick balancing: tuning Lévy flights to improve balance control. *Chaos* 14: 691–698, 2004.

Cluff T, Balasubramaniam R. Motor learning characterized by changing Lévy distributions. *PLoS One* 4: e5998, 2009.

Cluff T, Riley MA, Balasubramaniam R. Dynamical structure of hand trajectories during pole balancing. *Neurosci Lett* 464: 88–92, 2009.

Diedrichsen J, Shadmehr R, Ivry RB. The coordination of movement: optimal feedback control, and beyond. *Trends Cogn Sci* 14: 31–39, 2010.

Domkin D, Laczko J, Djupsjobacka M, Jaric S, Latash ML. Joint angle variability in 3D bimanual pointing: uncontrolled manifold analysis. *Exp Brain Res* 163: 44–57, 2005.

Domkin D, Laczko J, Jaric S, Johansson H, Latash ML. Structure of joint variability in bimanual pointing tasks. *Exp Brain Res* 143: 11–23, 2002.

Faisal AA, Selen LPJ, Wolpert DM. Noise in the nervous system. *Nat Rev Neurosci* 9: 292–303, 2008.

Flanagan JR, Lolley S. The inertial anisotropy of the arm is accurately predicted during movement planning. *J Neurosci* 21: 1361–1369, 2001.

Flanagan JR, Vetter P, Johansson RS, Wolpert DM. Prediction precedes control in motor learning. *Curr Biol* 13: 146–150, 2003.

Foo P, Kelso JAS, de Guzman GC. Functional stabilization of unstable fixed points: human pole balancing using time to balance information. *J Exp Psychol Hum Percept Perform* 26: 1281–1297, 2000.

Gabriel DA. Changes in kinematic and EMG variability while practicing a maximal performance task. *J Electromyogr Kinesiol* 12: 407–412, 2002.

Gribble PL, Scott SH. Overlap of internal models in motor cortex for mechanical loads during reaching. *Nature* 417: 938–941, 2002.

Holm S. A simple sequentially rejective multiple test procedure. *Scand Stat Theory Appl* 6: 65–70, 1979.

Jacobs RA. Adaptive precision pooling of model neuron activities predicts the efficiency of human visual learning. *J Vis* 22: 1–15, 2009.

Ko YG, Challis JH, Newell KM. Postural coordination patterns as a function of dynamics of the support surface. *Hum Mov Sci* 20: 737–764, 2001.

Konczak J, vander Velden H, Jaeger L. Learning to play the violin: motor control by freezing, not freeing degrees of freedom. *J Mot Behav* 41: 243–252, 2009.

Kurtzer IL, Pruszynski JA, Scott SH. Long-latency reflexes of the arm reflect an internal model of limb dynamics. *Curr Biol* 18: 449–453, 2008.

Lacquaniti F, Soechting JP. Coordination of arm and wrist movements during a reaching task. *Neuroscience* 2: 399–408, 1982.

Latash M. There is no motor redundancy in human movements. There is motor abundance. *Motor Control* 4: 259–261, 2000.

Latash ML, Scholz JP, Schoner G. Toward a new theory of motor synergies. *Motor Control* 11: 276–308, 2007.

Latash ML, Scholz JP, Schoner G. Motor control strategies revealed in the structure of motor variability. *Exerc Sport Sci Rev* 30: 26–31, 2002.

Loram ID, Gollee H, Lakie M, Gawthrop PJ. Human control of an inverted pendulum: is continuous control necessary? Is intermittent control effective? Is intermittent control physiological? *J Physiol* 589: 307–324, 2011.

Loram ID, Lakie M, Gawthrop P. Visual control of stable, and unstable loads: what is the feedback delay and extent of linear time-invariant control? *J Physiol* 587: 1343–1365, 2009.

Mah CD, Mussa-Ivaldi FA. Evidence for a specific internal representation of motion-force relationships during object manipulation. *Biol Cybern* 88: 60–72, 2003.

McDonald PV, van Emmerik REA, Newell KM. The effects of practice on limb kinematics in a throwing task. *J Mot Behav* 21: 245–264, 1989.

Mehta B, Schaal S. Forward models in visuomotor control. *J Neurophysiol* 88: 942–953, 2002.

Milton J, Cabrera JL, Ohira T, Tajima S, Tonosaki Y, Eurich CW, Campbell SA. The time-delayed inverted pendulum: implications for human balance control. *Chaos* 19: 026110, 2009.

Polit A, Bizzi E. Processes controlling arm movements in monkeys. *Science* 201: 1235–1237, 1978.

Ranganathan R, Newell KM. Motor synergies: feedback and error compensation within and between trials. *Exp Brain Res* 186: 561–570, 2008.

Scholz JP, Kang N, Patterson D, Latash ML. Uncontrolled manifold analysis of single trials during multi-finger force production by persons with and without Down syndrome. *Exp Brain Res* 153: 45–58, 2003.

Scholz JP, Schoner G. The uncontrolled manifold concept: identifying control variables for a functional task. *Exp Brain Res* 126: 289–306, 1999.

Scott SH. Optimal feedback control and the neural basis of volitional motor control. *Nat Rev Neurosci* 5: 532–546, 2004.

Southard D, Higgins T. Changing movement patterns: effects of demonstration, and practice. *Res Q Exerc Sport* 58: 77–80, 1987.

Temprado J, Della-Grasta M, Farrell M, Laurent M. A novice-expert comparison of (intra-limb) coordination subserving the volleyball serve. *Hum Mov Sci* 16: 653–676, 1997.

Timmann D, Citron R, Watts S, Hore J. Increased variability in finger position occurs throughout overarm throws made by cerebellar and unskilled subjects. *J Neurophysiol* 86: 2690–2702, 2001.

Todorov E, Jordan M. Optimal feedback control as a theory of motor coordination. *Nat Neurosci* 5: 1226–1235, 2002.

Treffner PJ, Kelso JAS. Dynamic encounters: long-term memory during functional stabilization. *Ecol Psychol* 11: 103–137, 1999.

Vereijken B, van Emmerik REA, Whiting HTA, Newell KM. Free(z)ing degrees of freedom in skill acquisition. *J Mot Behav* 24: 133–142, 1992.

Yang JF, Scholz JP. Learning a throwing task is associated with differential changes in the use of motor abundance. *Exp Brain Res* 163: 137–158, 2005.

Yen JT, Chang YH. Rate-dependent control strategies stabilize limb forces during human locomotion. *J R Soc Interface* 7: 801–810, 2010.

Young RP, Marteniuk RG. Stereotypic muscle-torque patterns are systematically adopted during acquisition of a multiarticular kicking task. *J Biomech* 31: 809–816, 1998.